Cardiovascular Research (2015) **107**, 184–196
doi:10.1093/cvr/cvv153

Late I_{Na} increases diastolic SR-Ca^{2+}-leak in atrial myocardium by activating PKA and CaMKII

Thomas H. Fischer[1], Jonas Herting[1], Fleur E. Mason[1], Nico Hartmann[1], Saera Watanabe[1], Viacheslav O. Nikolaev[1,2], Julia U. Sprenger[1], Peidong Fan[3], Lina Yao[3], Aron-Frederik Popov[4], Bernhard C. Danner[4], Friedrich Schöndube[4], Luiz Belardinelli[3], Gerd Hasenfuss[1,2], Lars S. Maier[5], and Samuel Sossalla[1,2]*

[1]Klinik für Kardiologie und Pneumologie/Herzzentrum, Georg-August-Universität Göttingen, Robert-Koch-Str. 40, 37075 Göttingen, Germany; [2]DZHK (German Center for Cardiovascular Research), partner site Göttingen, Göttingen, Germany; [3]Department of Biology, Cardiovascular, Therapeutic Area, Gilead Sciences, Foster City, CA, USA; [4]Klinik für Thorax-, Herz-, Gefäßchirurgie/Herzzentrum, Georg-August-Universität Göttingen, Göttingen, Germany; and [5]Innere Medizin II – Kardiologie, Universitätsklinikum Regensburg, Regensburg, Germany

Received 31 July 2014; revised 1 April 2015; accepted 16 April 2015; online publish-ahead-of-print 19 May 2015

Time for primary review: 38 days

Aims Enhanced cardiac late Na current (late I_{Na}) and increased sarcoplasmic reticulum (SR)-Ca^{2+}-leak are both highly arrhythmogenic. This study seeks to identify signalling pathways interconnecting late I_{Na} and SR-Ca^{2+}-leak in atrial cardiomyocytes (CMs).

Methods and results In murine atrial CMs, SR-Ca^{2+}-leak was increased by the late I_{Na} enhancer Anemonia sulcata toxin II (ATX-II). An inhibition of Ca^{2+}/calmodulin-dependent protein kinase II (Autocamide-2-related inhibitory peptide), protein kinase A (H89), or late I_{Na} (Ranolazine or Tetrodotoxin) all prevented ATX-II-dependent SR-Ca^{2+}-leak. The SR-Ca^{2+}-leak induction by ATX-II was not detected when either the Na^+/Ca^{2+} exchanger was inhibited (KBR) or in CaMKIIδc-knockout mice. FRET measurements revealed increased cAMP levels upon ATX-II stimulation, which could be prevented by inhibition of adenylyl cyclases (ACs) 5 and 6 (NKY 80) but not by inhibition of phosphodiesterases (IBMX), suggesting PKA activation via an AC-dependent increase of cAMP levels. Western blots showed late I_{Na}-dependent hyperphosphorylation of CaMKII as well as PKA target sites at ryanodine receptor type-2 (-S2814 and -S2808) and phospholamban (-Thr17, -S16). Enhancement of late I_{Na} did not alter Ca^{2+}-transient amplitude or SR-Ca^{2+}-load. However, upon late I_{Na} activation and simultaneous CaMKII inhibition, Ca^{2+}-transient amplitude and SR-Ca^{2+}-load were increased, whereas PKA inhibition reduced Ca^{2+}-transient amplitude and load and additionally slowed Ca^{2+} elimination. In atrial CMs from patients with atrial fibrillation, inhibition of late I_{Na}, CaMKII, or PKA reduced the SR-Ca^{2+}-leak.

Conclusion Late I_{Na} exerts distinct effects on Ca^{2+} homeostasis in atrial myocardium through activation of CaMKII and PKA. Inhibition of late I_{Na} represents a potential approach to attenuate CaMKII activation and decreases SR-Ca^{2+}-leak in atrial rhythm disorders. The interconnection with the cAMP/PKA system further increases the antiarrhythmic potential of late I_{Na} inhibition.

Keywords Late Na current • Antiarrhythmic drugs • Atrial fibrillation • Protein kinases • SR-Ca^{2+}-leak

1. Introduction

The late Na^+ current (late I_{Na}) is a small Na^+ inward current, which follows the peak Na^+ current, persists throughout the action potential[1] and plays a small electrophysiological role under physiological conditions. However, an enhanced late I_{Na} significantly contributes to total Na^+ influx.[2] Late I_{Na} was shown to be increased in ischemia[3] and oxidative stress[4] as well as in heart failure[5] and atrial fibrillation (AF).[6] Under these conditions, the total amount of Na^+ entering the cell via late I_{Na} can even exceed that of peak I_{Na}.[7] In addition, an increased late I_{Na} prolongs action potential duration (APD)[8] and promotes early afterdepolarizations (EADs).[9] EADs and triggered atrial activity

* Corresponding author. Tel: +49 551 399481; fax: +49 551 398941, Email: ssossalla@med.uni-goettingen.de

© The Author 2015. Published by Oxford University Press on behalf of the European Society of Cardiology.
This is an Open Access article distributed under the terms of the Creative Commons Attribution Non-Commercial License (http://creativecommons.org/licenses/by-nc/4.0/), which permits non-commercial re-use, distribution, and reproduction in any medium, provided the original work is properly cited. For commercial re-use, please contact journals.permissions@oup.com

constitute a pathomechanism for the initiation and perpetuation of AF.[10] Another relevant mechanism in AF is an increased SR-Ca^{2+}-leak,[11] which occurs when altered ryanodine receptor type-2 (RyR2) spontaneously opens in diastole releasing small amounts of Ca^{2+} (Ca^{2+} sparks). The increased diastolic Ca^{2+} leak in AF is caused by CaMKII-dependent hyperphosphorylation of RyR2, which triggers delayed afterdepolarizations (DADs) via activation of the Na^+/Ca^{2+} exchanger (NCX) leading to transient inward currents (I_{ti}).[12] Furthermore, it has been suggested that PKA-dependent phosphorylation of RyR2 decreases the amount of RyR2-bound calstabin-2 and also contributes to the instability of RyR2.[13] Thus, both arrhythmic triggers (increased late I_{Na} and increased SR-Ca^{2+}-leak) coexist in AF. This study investigates if both cellular phenomena are linked and elucidates the underlying pathways.

2. Methods

2.1 Human myocardial tissue

All procedures performed conform to the Declaration of Helsinki and were approved by the local ethics committee. Written informed consent was received from all participants prior to inclusion. Human atrial myocardium was obtained from resections of the left atrial appendage during open heart surgery. The samples were immediately placed in cooled cardioplegic solution (in mmol/L: NaCl 110, KCl 16, $MgCl_2$ 16, $NaHCO_3$ 16, $CaCl_2$ 1.2, and glucose 11) and kept cool until cell isolation started or instantly frozen in liquid nitrogen and stored at −80°C for western blot analysis.

2.2 Myocyte isolation

2.2.1 Mouse

The animal study was approved by the local or ethics review board and procedures were performed in accordance with the NIH guidelines (guide for the care and use of laboratory animals) and the guidelines from Directive 2010/63/EU of the European Parliament on the protection of animals used for scientific purposes.

Mice were killed in isoflurane 133 anaesthesia (5%) by cervical dislocation. To ensure sufficient digestion of atrial myocardium, mice were administered 100 IU heparin by an intraperitoneal injection prior to isolation. A Langendorff apparatus was used to retrogradely perfuse the explanted hearts with an initially Ca^{2+}-free solution containing (in mmol/L) NaCl 113, KCl 4.7, KH_2PO_4 0.6, $Na_2HPO_4{\cdot}2H_2O$ 0.6, $MgSO_4{\cdot}7H_2O$ 1.2, $NaHCO_3$ 12, $KHCO_3$ 10, HEPES 10, Taurine 30, 2,3-butanedione monoxime (BDM) 10, glucose 5.5, and phenol red 0.032 (37°C, pH 7.4). Then, 7.5 mg/mL of liberase 1 (Roche Diagnostics, Mannheim, Germany) and trypsin 0.6% (Life Technologies, Carlsbad, CA, USA) as well as 0.125 mmol/L of $CaCl_2$ were added to the perfusion solution. Once the tissue became flaccid, ventricular and atrial myocardium was separated by cutting off the atria above the atrioventricular valve level. The atrial myocardium was cut into small pieces and again dispersed in solution. Concentration of Ca^{2+} was stepwise increased every 7 min until desired concentration was reached. Cells were plated on laminin-coated recording chambers and left for 20 min to enable settling.

2.2.2 Human

Left atrial myocardium was rinsed, cut into small pieces and incubated at 37°C in a spinner flask filled with Ca^{2+}-free solution containing 1.0 mg/mL of collagenase (Worthington type 1, 185 U/mg), 0.05 mg/mL of proteinase (Life Technologies) and (in mmol/L): NaCl 88, sucrose 88, KCl 5.4, $NaHCO_3$ 4, NaH_2PO_4 0.3, MgCl 1, HEPES 10, Taurine 20, glucose 10, and sodium pyruvate 5 (pH 7.4). After 45 min, the supernatant was discarded and fresh Ca^{2+}-free solution containing only collagenase was added. The myocytes were incubated in the solution for 10–20 min and agitated using a Pasteur pipette. The supernatant containing dispersed cells was removed and centrifuged (59 *g*, 7 min). Fresh Ca^{2+}-free solution with collagenase was added to the remaining tissue. This procedure was repeated 4–5 times. After every step, the centrifuged cells were resuspended in KB medium containing (mmol/L): Taurine 10, glutamic acid 70, KCl 25, KH_2PO_4 10, dextrose 22, EGTA 0.5, and bovine calve serum 10% (pH 7.4, KOH, room temperature). Only cell solutions containing elongated cardiomyocytes (CMs) with clear cross striations were selected for experiments, plated on laminin-coated recording chambers, and left to settle for 30 min.

2.3 Patch-clamp experiments

Ruptured-patch whole-cell voltage-clamp experiments were used to measure late I_{Na} using microelectrodes (2–3 MΩ). Pipettes were filled with (in mmol/L) 95 CsCl, 40 Cs-glutamate, 10 NaCl, 0.92 $MgCl_2$, 5 Mg-ATP, 0.3 Li-GTP, 5 HEPES, 0.03 niflumic acid (to block Ca-activated chloride current), 0.02 nifedipine (to block Ca current), 0.004 strophanthidin (to block NCX current), 1 EGTA, and 0.36 $CaCl_2$ (free $[Ca^{2+}]_i$,100 nmol/L; pH 7.2, CsOH). The bath solution contained (in mmol/L) 135 NaCl, 5 tetramethylammonium chloride, 4 CsCl, 2 $MgCl_2$, 10 glucose, and 10 HEPES (pH 7.4, NaOH). To minimize contaminating Ca^{2+} currents during late I_{Na} measurements, Ca^{2+} was omitted from the bath solution. Anemonia sulcata toxin II (ATX-II; 0.5 nmol/L) vs. control was added to the bath solution. Access resistance was <7 MΩ. In all experiments, myocytes were mounted on the stage of a microscope (Nikon T 300). Fast capacitance was compensated in cell-attached configuration. Membrane capacitance and series resistance were compensated after patch rupture. Signals were filtered with 2.9 and 10 kHz Bessel filters and recorded with an EPC10 amplifier (HEKA Elektronik). Myocytes were held at −120 mV and late I_{Na} was elicited using a train of pulses to −35 mV (1000 ms duration, 10 pulses, and basic cycle length 2000 ms). Recordings were started 5 min after rupture. Experiments were conducted at room temperature. The measured current was integrated (between 50 and 100 ms) and normalized to the membrane capacitance.

For action potential recordings, ruptured-patch whole-cell voltage-clamp experiments were used to measure membrane potential (current-clamp configuration). For membrane potential measurements, microelectrodes were filled with (in mmol/L) 120 K-aspartate, 8 KCl, 7 NaCl, 1 $MgCl_2$, 10 HEPES, and 5 Mg-ATP (pH 7.2, KOH). The bath solution contained (mmol/L) 135 NaCl, 5.4 KCl, 1 $MgCl_2$, 1 $CaCl_2$, 10 glucose, and 10 HEPES (pH 7.4, NaOH). Action potentials were continuously elicited by square current pulses of 1–2 nA amplitude and 1–5 ms duration at 3 Hz. Access resistance was typically ∼20 MΩ after patch rupture. When appropriate, ATX-II (0.5 nmol/L) or ranolazine (10 μmol/L) was added to the bath solution. Fast capacitance was compensated in cell-attached configuration. Membrane capacitance and series resistance were compensated after patch rupture. Signals were filtered with 2.9 and 10 kHz Bessel filters and recorded with an EPC10 amplifier (HEKA Elektronik). Recordings were started 5 min after rupture. All experiments were conducted at room temperature.

2.4 Intracellular Ca^{2+} imaging

2.4.1 Confocal microscopy (measurement of SR Ca^{2+} sparks)

2.4.1.1 Mouse

Isolated CMs were incubated at room temperature for 30 min with a Fluo-3 AM loading buffer (10 μmol/L, Molecular Probes), which in the treatment groups contained ATX-II (0.5 nmol/L) alone or in combination with Ranolazine (10 μmol/L, Gilead Sciences, Palo Alto, CA, USA), CaMKII inhibitor Autocamide-2-related inhibitory peptide (AIP, 1 μmol/L, Alexis Corp., Switzerland), Tetrodotoxin (TTX, 2 μmol/L), or KBR (0.1 μmol/L). AIP was used in its myristoylated form to ensure cell permeability. Experimental solution contained (in mmol/L): KCl 4, NaCl 140, $MgCl_2$ 1, HEPES 5, glucose 10, $CaCl_2$ 2 (pH 7.4, NaOH, room temperature), and the respective active agents. Cells were continuously superfused during experiments. To wash out the loading buffer and remove any extracellular dye as well as to allow enough time for complete de-esterification of Fluo-3 AM, cells were superfused with experimental solution for 5 min before experiments were started. Ca^{2+} spark measurements were performed with a laser scanning

confocal microscope (LSM 5 Pascal, Zeiss) using a ×40 oil immersion objective. Fluo-3 was excited by an argon ion laser (488 nm) and emitted fluorescence was collected through a 505 nm long-pass emission filter. Fluorescence images were recorded in the line scan mode with 512 pixels per line (width of each scan line: 38.4 μm) and a pixel time of 0.64 μs. One image consists of 10 000 unidirectional line scans, equating to a measurement period of 7.68 s. Experiments were conducted at resting conditions after loading the SR with Ca^{2+} by repetitive field stimulation (at 3 Hz, 20 V). Typically shaped Ca^{2+} sparks were detected by eye and quantified by the program SparkMaster for ImageJ with the discrimination criterion 4.4 SD. The mean spark frequency of the respective cell (CaSpF) resulted from the number of sparks normalized to cell width and scan rate (100 $\mu m^{-1} s^{-1}$). Spark size (CaSpS) was calculated as the product of spark amplitude (F/F_0), duration, and width. From this, we inferred the average leak per cell by multiplication of CaSpS with CaSpF. For the illustration of detected Ca^{2+} sparks (*Figures 2A*, *3A*, *4A*, and *8A*), representative confocal line scans from each group were converted into a surface plot using ImageJ (*x*-axis = time; *y*-axis = width; *z*-axis = brightness, respective range of grey values as annotated).

2.4.1.2 Human

Isolated CMs were stained and measured as annotated above with the following differences: Fluo 3 AM loading buffer either contained Ranolazine (10 μmol/L), AIP (1 μmol/L), H89 (5 μmol/L), KBR (0.1 μmol/L), or no active agent. The experimental solution contained (in mmol/L): NaCl 136, KCl 4, NaH_2PO_4 0.33, $NaHCO_3$ 4, $CaCl_2$ 2, $MgCl_2$ 1.6, HEPES 10, glucose 10 (pH 7.4, NaOH, room temperature), and the respective active agents. Cells were stimulated at 1 Hz for 10 s (20 V) to ensure appropriate SR-Ca^{2+}-load before measurements were started.

2.4.2 Epifluorescence microscopy (systolic Ca^{2+} transients and SR Ca^{2+} content)

2.4.2.1 Mouse

CMs were isolated and plated as described above and incubated with a Fluo-4 AM loading buffer (10 μmol/L, Molecular Probes) for 15 min. In the intervention groups, the loading buffer also contained the respective active agents as described above for mouse/human confocal microscopic measurements. After staining, the CMs were superfused with experimental solution (as described in the section 'Confocal microscopy') for 5 min before measurements were started to enable complete de-esterification of intracellular Fluo-4 and allow cellular rebalance of Ca^{2+} cycling properties. During measurements, CMs were continuously superfused with experimental solution. Measurements were performed with a Nikon Eclipse TE2000-U microscope provided with a fluorescence detection system (ION OPTIX Corp.). Cells were excited at 480 ± 15 nm, and the emitted fluorescence was collected at 530 ± 20 nm. Systolic Ca^{2+} transients were recorded at steady-state conditions under constant field stimulation (1, 2, and 4 Hz). To assess the SR Ca^{2+} content, the amplitude of caffeine-induced Ca^{2+} transients was measured. After stopping the stimulation during steady-state conditions at 1 Hz, caffeine (10 mmol/L, Sigma-Aldrich, St Louis, MO, USA) was applied directly onto the cell, leading to immediate and complete SR Ca^{2+} release. The recorded Ca^{2+} transients were analysed with the software IONWizard^R (ION OPTIX Corp.). For the evaluation of the speed of Ca^{2+} reuptake into the SR, the decay constant *k* (reciprocal of Tau) of caffeine-induced Ca^{2+} transients was subtracted from the decay constant *k* of systolic Ca^{2+} transients at 1 Hz ($k_{sys} - k_{caff}$).

2.5 Western blots

Mouse hearts were rapidly removed and immersed in oxygenated Krebs–Henseleit buffer (in mmol/L: NaCl 118, KCl 4.8, KH_2PO_4 1.2, $CaCl_2$ 2.5, $MgSO_4$ 1.2, pyruvic acid 2, glucose 5.5, Na_2EDTA 0.5, and $NaHCO_3$ 25, pH 7.4). Mouse right atria were quickly excised and suspended in a chamber of the Danish Myo Technologies (DMT) myograph containing 8 mL of oxygenated Krebs–Henseleit buffer at 37°C. The spontaneously beating right atria were preincubated with late Na^+ current, CaMKII, or PKA inhibitors for 30 min, and then incubated with 0.5 nmol/L of ATX-II for an additional 30 min. The atria were then snap-frozen in liquid nitrogen and stored at −80°C. Atria were lysed with Tissue Lyser (Qiagen, Valencia, CA, USA) in 0.2 mL of lysis buffer containing 20 mmol/L of Tris, pH 7.5, 2 mmol/L of EDTA, 10 mmol/L of EGTA, 0.25 mmol/L of sucrose, 1% Triton X-100, and 1 tablet of protease inhibitor/10 mL (Sigma, St Louis, MO, USA). Lysates were incubated on ice for 20 min and then centrifuged at 9408 *g* for 5 min at 4°C. The supernatant was saved. About 20 μg of protein was loaded with SDS sample buffer, run on a 10% SDS–PAGE, transferred, and probed for phospho-CaMKII at threonine 287 and GAPDH (Santa Cruz Biotechnology, Santa Cruz, CA, USA), phospho-phospholamban (PLN) at threonine 16, phospho-PLN at threonine 17, phospho-RyR2 at serine 2808, and phospho-RyR2 at serine 2814 (Badrilla, Leeds, UK). Secondary antibody was horseradish peroxidase-linked goat anti-rabbit (1 : 1000; PerkinElmer Life and Analytical Sciences, Waltham, MA, USA). The intensity of individual bands from western blots was quantified using ImageJ software, normalized to GAPDH, and then shown relative to the control group value.

2.6 FRET measurements and data analysis

Freshly isolated adult mouse atrial CMs from EPAC1-camps mice were plated onto laminin-coated coverslides and allowed to settle for 30 min. Subsequently, coverslides with isolated CMs were mounted in an imaging chamber (Attofluor cell chamber, Invitrogen) equipped with an electrode. After washing the cells once with Tyrode solution (in mmol/L: KCl 1, NaCl 149, $MgCl_2$ 1, HEPES 5, glucose 10, and $CaCl_2$ 1, pH 7.54), 400 μL of Tyrode solution was added to the chamber. The cells were preincubated for 7 min with Tyrode solution containing IBMX (Applichem, 0.1 mmol/L), NKY80 (Sigma-Aldrich, 0.01 mmol/L), KBR (0.1 μmol/L), or no inhibitor in the control group. Subsequently, myocytes were field-stimulated at 1 Hz and FRET measurements (Förster resonance energy transfer) were performed using an inverted fluorescent microscope (Nikon T*i*) and the MicroManager software. The FRET donor cyan fluorescent protein (CFP) was excited at 440 nm using a CoolLED light source. Images were acquired every 5 s in CFP and YFP emission channels, with an exposure time of usually 10 ms as described. The compounds were diluted in Tyrode solution. ATX-II (0.5 nmol/L) was added to the imaging chamber 50 s after the start of the measurements, and 100 nmol/L of isoprenaline was added after the ATX-II reaction reached a stable plateau, usually after 5 min. FRET data analysis was performed using the Origin 8.5 software as previously described. To calculate the corrected FRET ratio, we subtracted the bleedthrough of the donor fluorescence (CFP) into the acceptor (YFP) channel using the equation: FRET ratio = (YFP − 0.63 × CFP)/CFP, where 0.63 is a bleed-through coefficient measured in cells expressing CFP only and normalized the values to the initial FRET ratio recorded at the beginning of every experiment. These data are presented as YFP/CFP ratio (norm.) in the results.

2.7 Statistical analysis

All data are presented as mean ± SEM. Student's *t*-test was used except for *Figures 1D* and *7D* (two-way ANOVA with the Bonferroni *post hoc* test). Values with $P < 0.05$ were considered as statistically significant.

3. Results

3.1 Effects of late I_{Na} modulation and CaMKII inhibition on SR-Ca^{2+}-leak

Atrial CMs isolated from hearts of wild-type (WT) mice were treated with Anemonia sulcata toxin II (ATX-II, 0.5 nmol/L), which led to an increase of the late I_{Na} integral by 53 ± 16% compared with untreated control (patch-clamp $P < 0.05$, *Figure 1 A* and *B*). The duration of the action potential (APD90) was prolonged by ∼1.8-fold by ATX-II

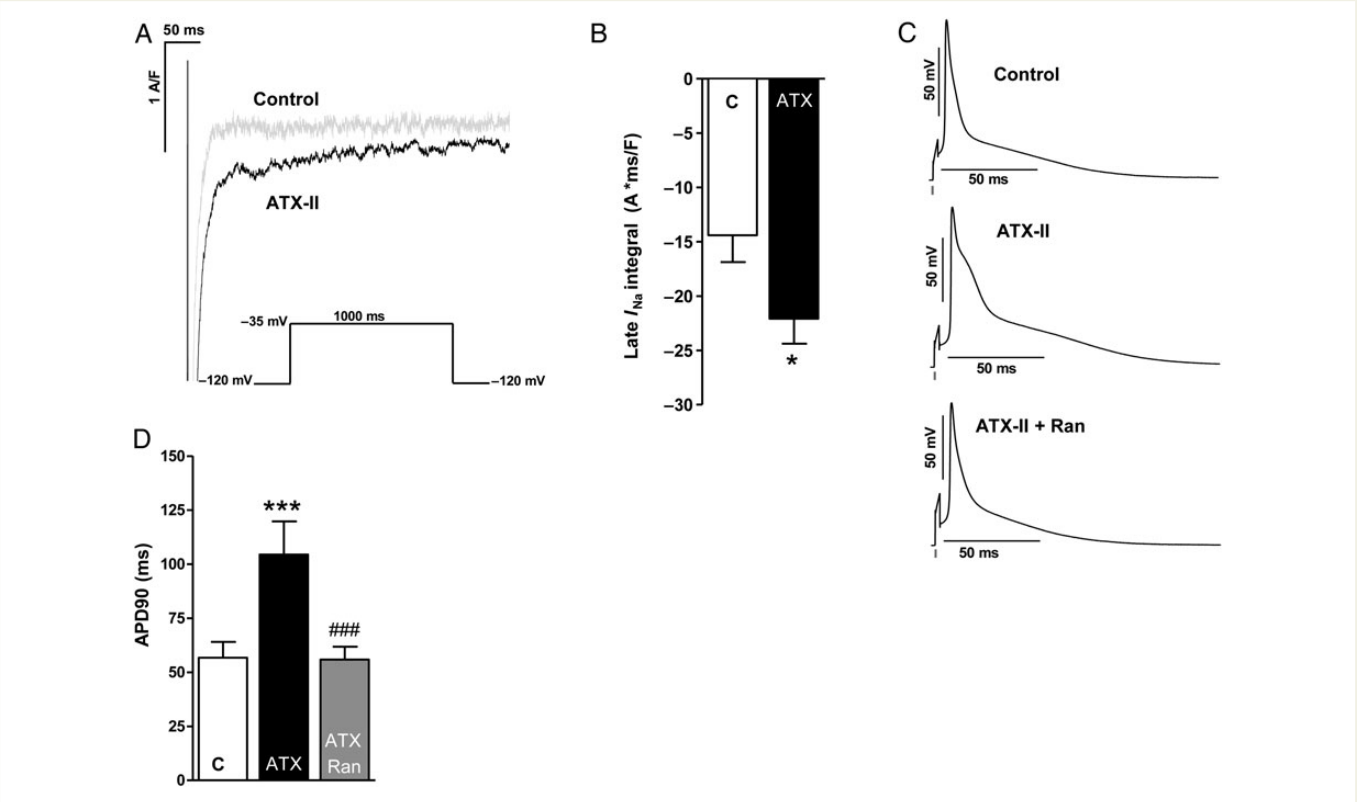

Figure 1 Effects of ATX-II treatment (0.5 nmol/L) on late I_{Na} of murine atrial CMs. (*A*) Representative original patch-clamp recordings of late Na^+ currents. (*B*) Mean values of late I_{Na} integral 50–100 ms (*n* mice/cells = 8/17 vs. 8/23). (*C*) Original recordings of action potentials (3 Hz) of untreated murine atrial CMs (above) as well as upon treatment with ATX-II (0.5 nmol/L, middle) and ATX-II + Ranolazine (10 μmol/L, below). (*D*) Quantification of action potential duration (APD90) after wash-in of ATX-II and Ranolazine (*n* mice/cells = 6/12 each). *significant vs. control; #significant vs. ATX-II; $^{*/\#}P < 0.05$; $^{**/\#\#}P < 0.01$; $^{***/\#\#\#}P < 0.001$.

(APD90 ATX-II vs. control = 104 ± 15 vs. 56 ± 6 ms, *Figure 1C* and *D*, $P < 0.001$). This effect could be antagonized by additional treatment with the late I_{Na} inhibitor Ranolazine (10 μmol/L; *Figure 1C* and *D*).

To evaluate the resulting effects on SR-Ca^{2+}-leak, atrial CMs of WT mice were field-stimulated and scanned for diastolic Ca^{2+} sparks. The basal Ca^{2+} spark frequency (CaSpF, 0.65 ± 0.09 100 μm^{-1} s^{-1}) was increased by ATX-II (0.5 nmol/L) to 1.22 ± 0.13 100 μm^{-1} s^{-1} (by 78 ± 44%, *Figure 2A* and *B*, $P < 0.001$). In addition, the amplitude of Ca^{2+} sparks was increased upon ATX-II treatment by 7 ± 1% (*Figure 1C*, $P < 0.001$) and the size of detected Ca^{2+} sparks was also increased (data not shown). Conclusively, the resulting calculated SR-Ca^{2+}-leak (CaSpF × Ca^{2+} spark duration × width × amplitude) was increased 2.4-fold (*Figure 2D*, $P < 0.001$). Accordingly, inhibition of late I_{Na} with Ranolazine (10 μmol/L) prevented the ATX-II-induced increase in CaSpF (*Figure 2B*, ATX-II + Ran vs. ATX-II, $P < 0.01$) and SR-Ca^{2+}-leak (*Figure 2D*, reduced by 49 ± 10% compared with ATX-II alone, $P < 0.01$). To exclude unspecific actions of Ranolazine, we additionally used the Na^+ channel blocker TTX (2 μmol/L) in combination with ATX-II (*Figure 2E–G*), which also reversed the ATX-II effect on SR-Ca^{2+}-leak (*Figure 2G*, $P < 0.001$) and increased spark amplitude (*Figure 2F*, $P < 0.01$). Interestingly, simultaneous CaMKII inhibition (AIP, 1 μmol/L, *Figure 2A–D*) as well as an inhibition of NCX (KBR, *Figure 3A–D*) also prevented the ATX-II-induced increase of CaSpF ($P < 0.001$ each) and SR-Ca^{2+}-leak ($P < 0.05$ and < 0.01, respectively), suggesting that CaMKII is activated via NCX-dependent Ca^{2+} overload. Importantly, ATX-II did not induce SR-Ca^{2+}-leak in atrial CMs of CaMKIIδc-knockout mice (CKO) (*Figure 3E* and *F*, $P = 0.46$).

3.2 Effects of late I_{Na} modulation and PKA inhibition on SR-Ca^{2+}-leak

Of note, an inhibition of PKA (H89 5 μmol/L) as well as an inhibition of both kinases (H89 5 μmol/L + AIP 1 μmol/L) also attenuated the ATX-II induced increase of CaSpF (*Figure 4B*, CaSpF control vs. ATX vs. ATX + H89 vs. ATX + H89 + AIP = 0.22 ± 0.05 vs. 1.01 ± 0.20 vs. 0.53 ± 0.17 vs. 0.57 ± 0.13 100 μm^{-1} s^{-1}) and significantly reduced the calculated SR-Ca^{2+}-leak compared with sole ATX-II treatment (*Figure 4D*, $P < 0.05$ each). PKA inhibition additionally reduced the amplitude of detected Ca^{2+} sparks (*Figure 4C*, $P < 0.05$).

3.3 Effects of late I_{Na} augmentation on intracellular cAMP levels

As PKA is activated by cAMP, we measured cytoplasmic cAMP levels upon ATX-II treatment in atrial CMs of EPAC-camps transgenic mice.[14] Indeed, ATX-II (0.5 nmol/L) increased cAMP levels (FRET ratio ATX-II vs. control = 0.96 ± 0.0047 vs. 1.0 ± 0.007; $P < 0.001$, *Figure 5A* and *E*). This response made up for ~28% of the maximal

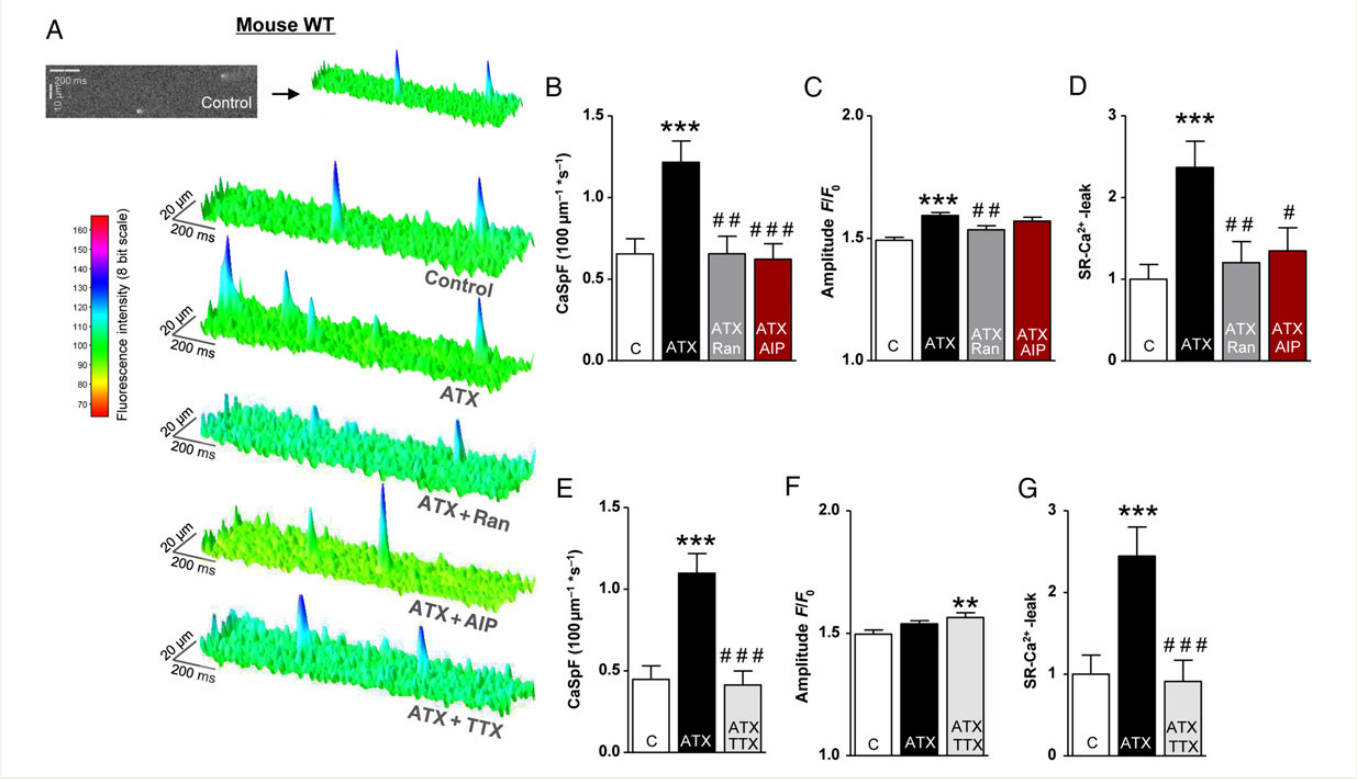

Figure 2 Effects of late I_{Na} modulations and CaMKII inhibition on SR-Ca^{2+}-leak in atrial CM of WT mice. (*A*) Surface plot of representative confocal line scans. (*B*–*G*) Mean values of CaSpF, Ca^{2+} spark amplitude, and the total calculated SR-Ca^{2+}-leak in the presence of the respective drugs (*B*–*D*: *n* mice/cells = 6/122 vs. 6/123 vs. 6/108 vs. 6/119; *E*–*G*: *n* = 5/89 vs. 5/93 vs. 5/92). *significant vs. control; #significant vs. ATX-II. $^{*/\#}P < 0.05$; $^{**/\#\#}P < 0.01$; $^{***/\#\#\#}P < 0.001$.

isoproterenol response (FRET ratio Iso 100 nmol/L vs. control = 0.88 ± 0.013 vs. 1.0 ± 0.0017; $P < 0.001$, *Figure 5A*). When we pre-incubated atrial CMs with the unselective phosphodiesterase (PDE) inhibitor IBMX (100 µmol/L, *Figure 5B*), the normalized YFP/CFP ratio upon ATX-II was still lowered compared to control (YFP/CFP ratio = 0.976 ± 0.005 vs. 1.0 ± 0.001, $P < 0.001$) and did not differ from untreated CMs exposed to ATX-II (YFP/CFP ratio = 0.964 ± 0.05). However, an inhibition of adenylyl cyclase (AC) isoforms AC5 and AC6 (NKY80, 10 µmol/L)[15] attenuated the cAMP response to ATX-II (*Figure 5C* and *E*; YFP/CFP ratio NKY80 + ATX vs. ATX = 0.988 ± 0.02 vs. 0.964 ± 0.05, $P < 0.001$). Of note, the preincubation with the reverse mode NCX inhibitor KBR (0.1 µmol/L) also reduced ATX-II-induced cAMP production (*Figure 5D* and *E*; YFP/CFP ratio ATX-II + KBR vs. ATX-II = 0.982 ± 0.004 vs. 0.964 ± 0.005, $P = 0.01$).

3.4 Effects of late I_{Na} modulation on phosphorylation of key Ca^{2+}-handling proteins

To further investigate the roles of CaMKII and PKA, we performed Western blots from extracted right murine atria that had been perfused with ATX-II and the respective inhibitors (*Figure 6* and see Supplementary material online, *Figure S1*). An augmentation of late I_{Na} (ATX-II, 0.5 nmol/L) increased the phosphorylation of CaMKII target sites PLN-T17 and RyR2-S2814 (*Figure 6A* and *B*, $P < 0.05$ each). In addition, CaMKII autophosphorylation at T287 was increased ($P < 0.05$). The hyperphosphorylation of CaMKII targets could be prevented by Ran (10 µmol/L), TTX (2 µmol/L), and AIP (1 µmol/L), but not by H89 (5 µmol/L; *Figure 6A* and *B*, $P < 0.05$ each).

Similarly, PKA targets PLN-S16 and RyR2-S2808, were hyperphosphorylated in ATX-II-treated atrial myocardium vs. control ($P < 0.05$), which could be prevented by treatment with Ranolazine, TTX, or H89, but not with AIP (*Figure 6A* and *B*, $P < 0.05$ each).

3.5 Effects of late I_{Na} modulation and CaMKII/PKA inhibition on Ca^{2+} kinetics and SR-Ca^{2+}-load

ATX-II treatment did not alter systolic Ca^{2+}-transient amplitude (*Figure 7A*—left and *B*, $P = 0.97$) or SR-Ca^{2+} -load (*Figure 7A*—right and *C*; $P = 0.35$). Different stimulation frequencies showed similar results (*Figure 7D*). Simultaneous CaMKII inhibition, however, increased systolic Ca^{2+}-transient amplitude at 2 Hz (*Figure 7B*, increased by 28 ± 7%, $P < 0.001$) and SR-Ca^{2+}-load (increased by 22 ± 9% vs. control, *Figure 7C*, $P < 0.05$), suggesting that late I_{Na} activates SR refill independently of CaMKII, which maintains SR-Ca^{2+}-load despite a markedly increased SR-Ca^{2+}-leak (ATX-II vs. control, *Figures 2D* and *7C*) and even leads to increased SR-Ca^{2+}-load and Ca^{2+}-transient amplitude when the CaMKII-dependent leak induction is prevented (ATX + AIP vs. control; *Figures 2D* and *7B* and *C*). This hypothesis was confirmed in CaMKII-knockout mice. Here, the treatment with ATX-II also increased SR-Ca^{2+} load (by 37 ± 9%, *Figure 7G* and *H*, $P < 0.05$). In contrast, the inhibition of PKA (ATX + H89) decreased

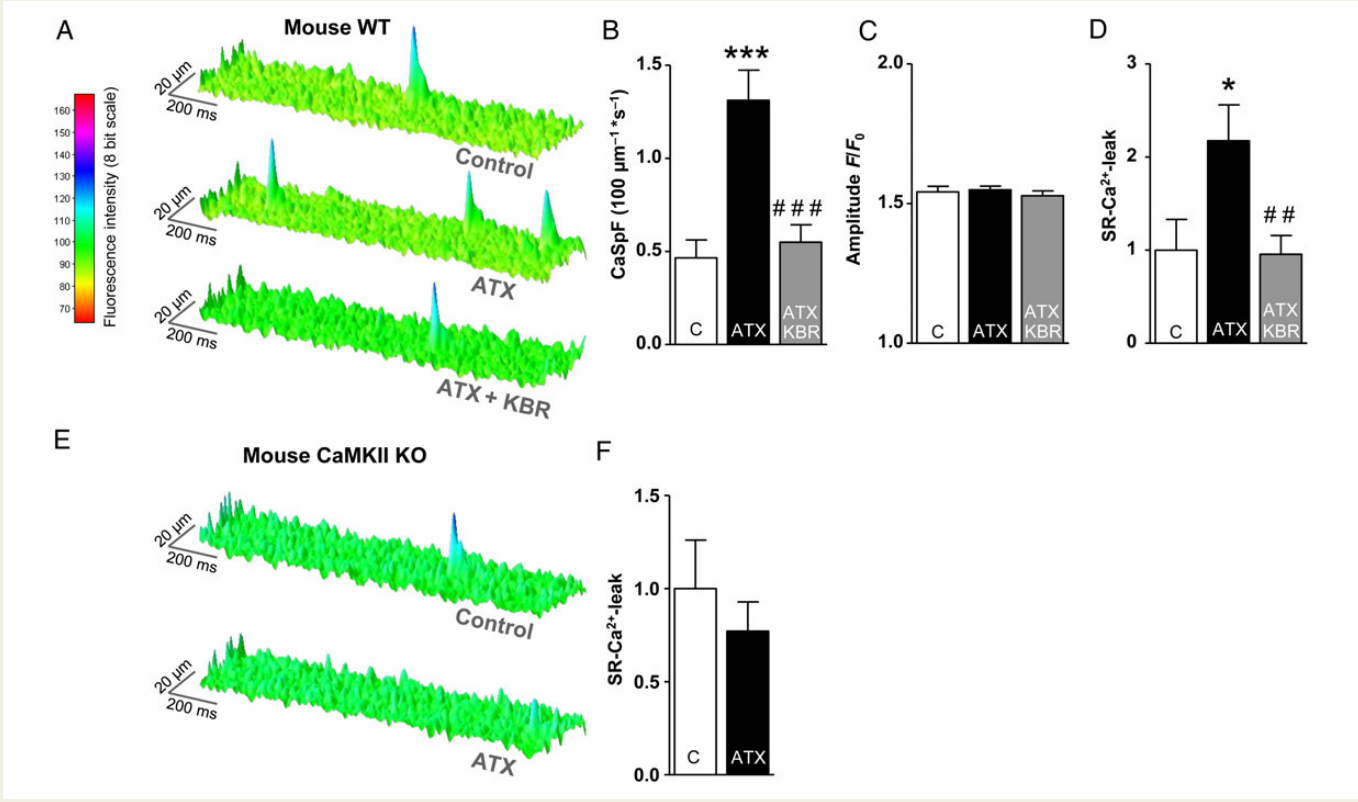

Figure 3 The impact of NCX inhibition and CaMKIIδc-KO on ATX-II-mediated induction of the SR-Ca^{2+}-leak in murine atrial CMs. (*A*) Surface plot of representative confocal line scans. (*B–D*) Mean values of the diastolic CaSpF, spark amplitude, and the SR-Ca^{2+}-leak (*n* mice/cells = 5/71 vs. 5/61 vs. 5/75). (*E*) Representative confocal line scans of atrial CM from CaMKIIδc-KO mice. (*F*) Mean values of the SR-Ca^{2+}-leak ($n = 5/148$ vs. 5/140, $P = 0.40$). *significant vs. control; #significant vs. ATX-II. $^{*/\#}P < 0.05$; $^{**/\#\#}P < 0.01$; $^{***/\#\#\#}P < 0.001$.

Ca^{2+}-transient amplitude at 2 Hz (*Figure 7B*, $P < 0.01$) and SR-Ca^{2+}-load (*Figure 7C*, $P < 0.001$). Furthermore, Ca^{2+} elimination kinetics were assessed. As a measure for the speed of Ca^{2+} uptake into the SR, the decay constant *k* of caffeine-induced Ca^{2+} transients (Ca^{2+} elimination predominantly via NCX) was subtracted from the decay constant of systolic transients (Ca^{2+} elimination via SERCA + NCX). Interestingly, ATX-II treatment did not significantly alter $k_{sys} - k_{caff}$ (*Figure 7E*, $P = 0.15$). Additional inhibition of CaMKII, however, yielded an acceleration of Ca^{2+} reuptake into the SR ($k_{sys} - k_{caff}$ ATX + AIP vs. control, increased by 34 ± 7%; $P < 0.05$). In contrast, inhibition of PKA decelerated SR reuptake (ATX + H89 vs. control, decreased by 33 ± 6%; $P < 0.001$). Moreover, ATX-II treatment increased the fractional Ca^{2+} release (*Figure 7F*, ratio $F/F_0/F/F_0$ caff, ATX-II vs. control = 0.80 ± 0.02 vs. 0.73 ± 0.02, $P < 0.01$), which was counteracted by PKA inhibition but not by CaMKII inhibition (*Figure 7F*).

3.6 Effects of late I_{Na}, CaMKII, and PKA inhibition in human AF

In human isolated left atrial CMs from patients with permanent AF (for patient characteristics see *Table 1*), inhibition of late I_{Na} (Ranolazine, 10 µmol/L) reduced CaSpF (*Figure 8B*, CaSpF Ran vs. control = 0.27 ± 0.10 vs. 0.63 ± 0.12 100 μm^{-1} s^{-1}, $P < 0.05$) and reduced amplitude, width, and duration of Ca^{2+} sparks (data not shown, $P < 0.001$ each). This translated into a robust reduction of the SR-Ca^{2+}-leak (*Figure 8B*, reduction by 88 ± 4%, $P < 0.01$). CaMKII inhibition (AIP 1 µmol/L) diminished CaSpF by 61 ± 9% (AIP vs. control = 0.34 ± 0.11 vs. 1.16 ± 0.26 100 μm^{-1} s^{-1}, $P < 0.01$, *Figure 8C*) and reduced SR-Ca^{2+}-leak by 69 ± 16% (*Figure 8C*, $P < 0.05$). Similar results were obtained upon PKA inhibition. The treatment of human AF CMs with H89 (5 µmol/L) significantly reduced the CaSpF by 66 ± 11% (*Figure 8D*, $P < 0.01$). This led to a reduction of calculated SR-Ca^{2+}-leak ($P < 0.05$). Additionally, inhibition of reverse-mode NCX with KBR (0.1 µmol/L) also suppressed diastolic RyR2 leakiness in human AF (*Figure 8E*, CaSpF KBR vs. control = 0.33 ± 0.08 vs. 0.68 ± 0.12 100 μm^{-1} s^{-1}, $P < 0.05$).

4. Discussion

The present data show for the first time that an enhancement of late I_{Na} potently induces SR-Ca^{2+}-leak in atrial CMs due to (i) an activation of CaMKII, which promotes diastolic RyR2 openings by hyperphosphorylation of RyR2 (Ser2814) and (ii) an activation of PKA (stimulation of AC 5/6 and increase of cAMP), which subsequently facilitates SR-Ca^{2+}-accumulation by increased phosphorylation of PLN (Ser16). Importantly, both kinases are necessary for late I_{Na}-dependent SR-Ca^{2+}-leak induction.

4.1 Late I_{Na} potently induces SR-Ca^{2+}-leak

To our knowledge, no direct measurements of SR-Ca^{2+}-leak as a function of late I_{Na} have been performed in atrial CMs. There is evidence in

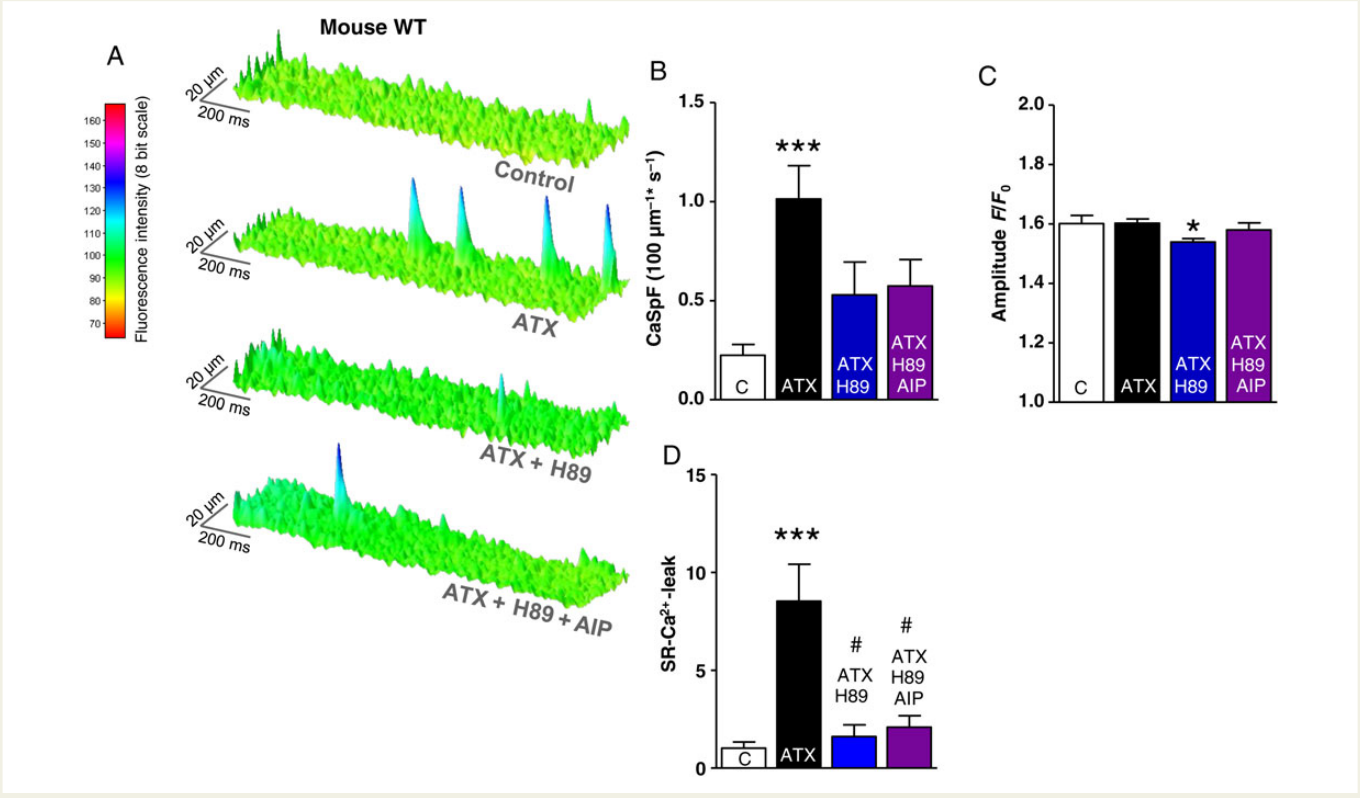

Figure 4 Effects of late I_{Na} modifications and PKA inhibition on SR-Ca^{2+}-leak in murine atrial CMs. (*A*) Surface plot of representative confocal line scans. (*B–D*) Mean values of the diastolic CaSpF, spark amplitude, and SR-Ca^{2+}-leak (*n* mice/cells = 6/100 vs. 6/87 vs. 4/33 vs. 3/47). *significant vs. control; #significant vs. ATX-II; $^{*/\#}P < 0.05$; $^{**/\#\#}P < 0.01$; $^{***/\#\#\#}P < 0.001$.

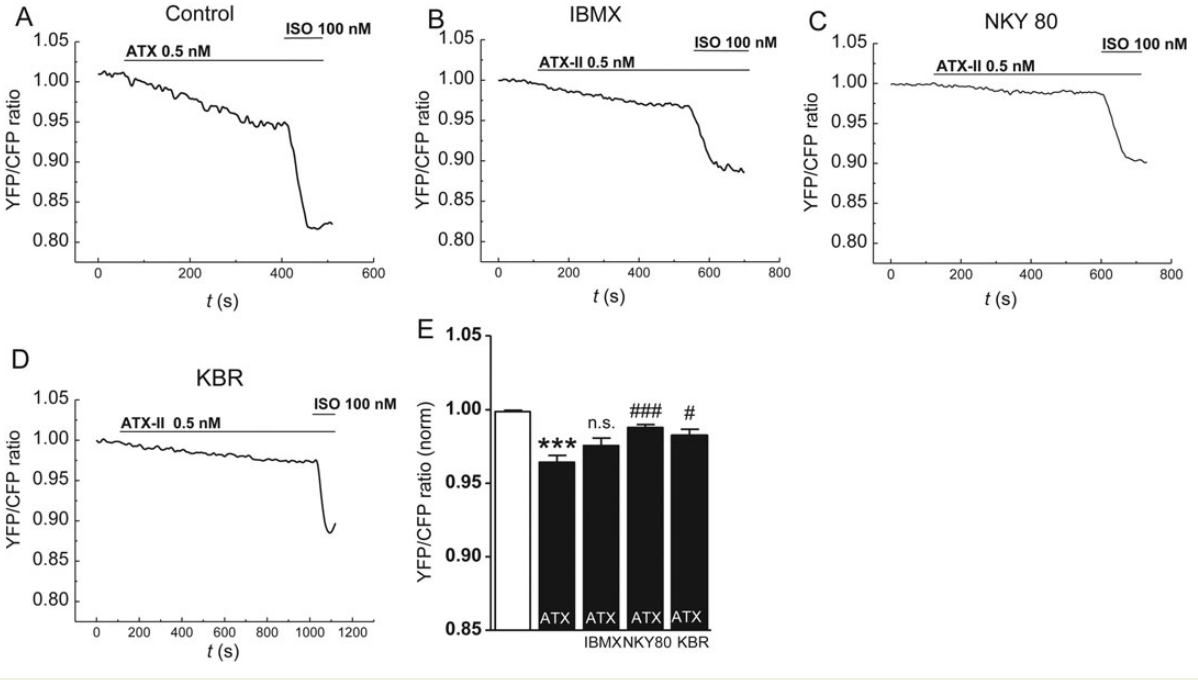

Figure 5 Effects of late I_{Na} induction on cellular cAMP levels in atrial CMs of mice. (*A–D*) YFP/CFP tracings in CMs of EPAC-camps transgenic mice upon ATX-II (0.5 nmol/L) and subsequent isoproterenol treatment (100 nmol/L). CMs were preincubated with a (*B*) PDE inhibitor IBMX (100 µmol/L), (*C*) an inhibitor of AC 5/6 (NKY80, 10 µmol/L), (*D*) an inhibitor of reverse-mode NCX KBR (0.1 µmol/L), or (*A*) no inhibitor. (*E*) Quantification of response of YFP/CFP ratio (*n* mice/cells = 10/39 vs. 3/8 vs. 3/10 vs. 3/11). *significant vs. steady-state before ATX-II; #significant vs. YFP/CFP ratio upon ATX-II in the control group. $^{*/\#}P < 0.05$; $^{**/\#\#}P < 0.01$; $^{***/\#\#\#}P < 0.001$.

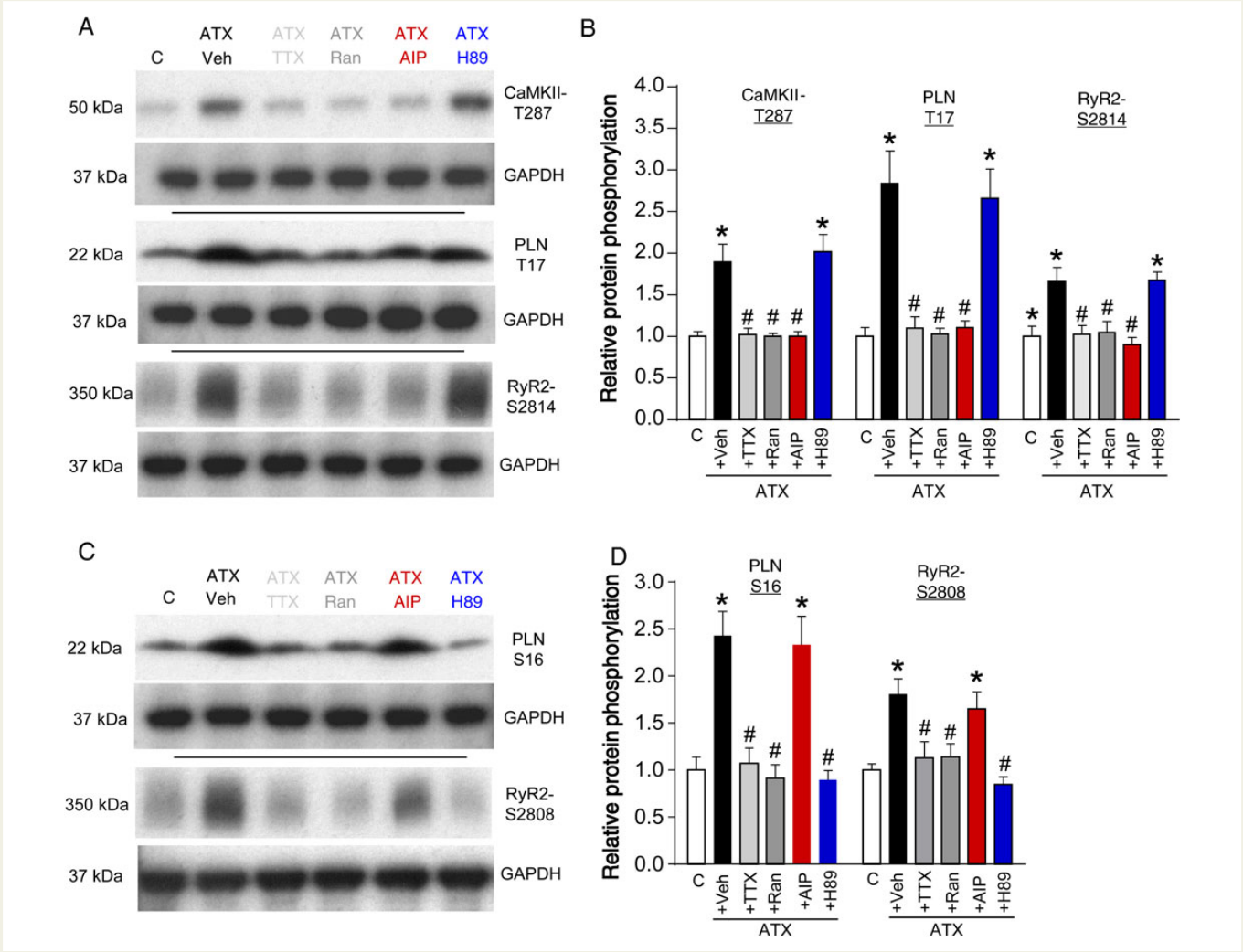

Figure 6 Phosphorylation of CaMKII and PKA targets in murine atria upon modulations of late I_{Na}. Representative western blots of the phosphorylation status of (*A*) CaMKII and (*C*) PKA targets. (*B* and *D*) Western blot quantifications of the respective groups (n mice = 4 and $P < 0.05$ each). *significant vs. control; #significant vs. ATX-II + Veh (vehicle).

the literature that an enhanced late I_{Na} induces spontaneous diastolic depolarizations derived from both EADs and DADs. An interference of late I_{Na} with Ca^{2+} cycling properties has been suggested.[16] However, the molecular basis of DADs downstream of an elevated Na^+ influx is unknown. It is generally agreed that DADs arise from cytoplasmic Ca^{2+} overload leading to electrogenic extrusion of Ca^{2+} from the cell via NCX. Cytoplasmic Ca^{2+} overload might be explained by facilitation of Ca^{2+} channel reactivation due to late I_{Na}-induced APD prolongation,[17] but increased SR-Ca^{2+}-leak may also play a role. We used ATX-II to increase late I_{Na}[18] and found the late I_{Na} integral to be increased by ~65% upon ATX-II in our setting. We found that an enhancement of late I_{Na} increases SR-Ca^{2+}-leak, but does not alter SR-Ca^{2+}-load. The effects of ATX-II seem to be late I_{Na}-related as they can be blocked by Ranolazine and TTX. Importantly, ATX-II-treated murine atrial CMs showed similar CaSpF as human atrial CMs isolated from patients with permanent AF. In summary, our findings show the interdependence of Na^+ current and Ca^{2+}-cycling abnormalities in atrial CMs. This mechanism may significantly contribute to the increased SR-Ca^{2+}-leak and cellular Ca^{2+} overload reported in human AF.[11,12]

4.2 Late I_{Na} activates CaMKII via a NCX-dependent mechanism

Hyperphosphorylation of RyR2 at S2814/2815 (mouse/human) has been shown to increase SR-Ca^{2+}-leak in ventricular[19] as well as in atrial myocardium.[11,12] Our study extends molecular findings, suggesting that late I_{Na} activates CaMKII in rat ventricular CMs,[20] to atrial myocardium. Of note, measurements of RyR2 function have not yet been performed in this context, either in ventricular or in atrial myocardium.[20]

Our data additionally show that CaMKII is essential for late I_{Na}-dependent SR-Ca^{2+}-leak induction as it can be effectively prevented by the specific CaMKII inhibitor AIP and an elevated late I_{Na} failed to increase SR-Ca^{2+}-leak in CaMKII-knockout mice. We further used KBR to inhibit the reverse mode of NCX function,[21] which also suppressed SR-Ca^{2+}-leak induction. It can thus be assumed that CaMKII is activated by Ca^{2+}, which has entered the cell via NCX in the setting of Na^+ overload. This mechanism may be pronounced in AF where NCX function is increased.[12] Of note, it was shown that CaMKII, in turn, can phosphorylate $Na_v1.5$, which enhances Na^+ influx via late I_{Na}.[22] Thus, cytoplasmic ion imbalance may establish a vicious circle

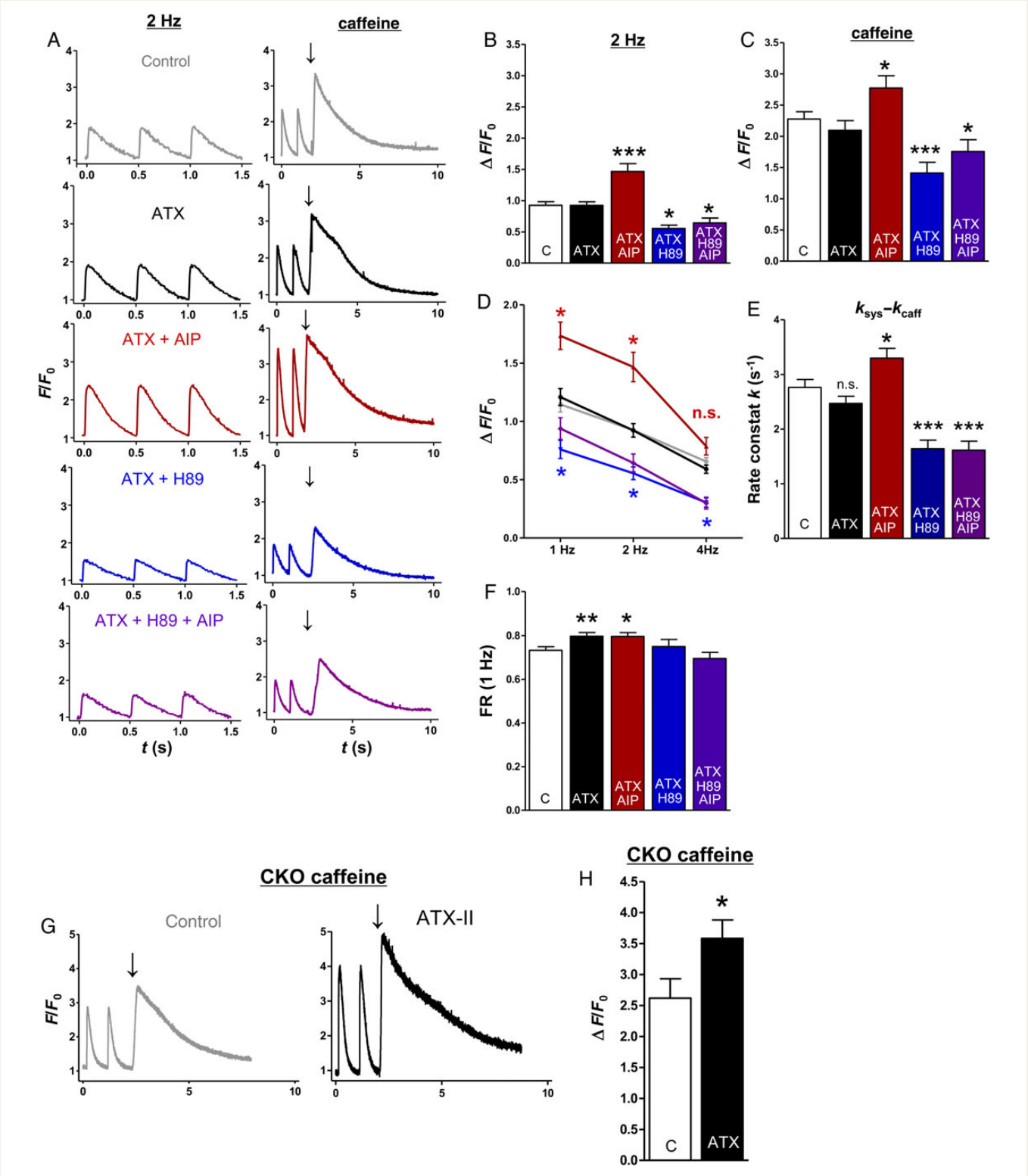

Figure 7 The impact of late I_{Na} modifications and CaMKII/PKA inhibition on stimulated and caffeine-induced Ca^{2+} transients of murine atrial CMs. (*A*) Representative original recordings (2 Hz, left) and caffeine-induced Ca^{2+} transients (right, arrow indicates caffeine application, WT). (*B*) Mean values of the amplitude ($\Delta F/F_0$) of stimulated Ca^{2+} transients (*n* mice/cells = 12/65 vs. 11/52 vs. 5/29 vs. 4/16 vs. 4/13 for *B*, *D*, *E*, and *F*). (*C*) Mean values of caffeine-induced Ca^{2+} transients ($\Delta F/F_0$; $n = 10/42$ vs. 11/37 vs. 5/27 vs. 4/15 vs. 4/13). (*D*) Mean values of Ca^{2+}-transient amplitudes ($\Delta F/F_0$) at different stimulation frequencies. (*E*) Mean values of Ca^{2+}-reuptake speed into the SR ($k_{sys} - k_{caff}$). (*F*) Mean values of fractional Ca^{2+} release (FR, $\Delta F/F_0$ 1 Hz/SR-Ca^{2+}-load). (*G*) Representative original recordings of atrial CMs from CaMKIIδc-KO mice (arrow indicates caffeine application). (*H*) Mean values of caffeine-induced Ca^{2+} transients in CaMKIIδc-KO mice ($n = 3/19$ vs. 3/22; $P < 0.05$). *significant vs. control. $^{*/\#}P < 0.05$; $^{**/\#\#}P < 0.01$; $^{***/\#\#\#}P < 0.001$.

Table 1 Characteristics of the patients from which human left atrial CMs were obtained

n	Male (%)	Age (years)	AF (%)	LVEF (%)	ICM (%)	Diabet (%)	β-Block (%)	ACE-I (%)	Amiod (%)	Digit (%)	CCB (%)
13	54.0	73.3 ± 1.8	100	50.6 ± 4.7	53.8	30.8	80.0	90.0	30.0	40.0	20.0

AF, atrial fibrillation; LVEF, left ventricular ejection fraction; ICM, ischaemic heart disease; Diabet, diabetes mellitus; β-block, β-blocker; ACE-I, ACE inhibitor; Amiod, Amiodarone; Digit, digitalis (Digoxin or Digitoxin); CCB, Ca^{2+} channel blockers.

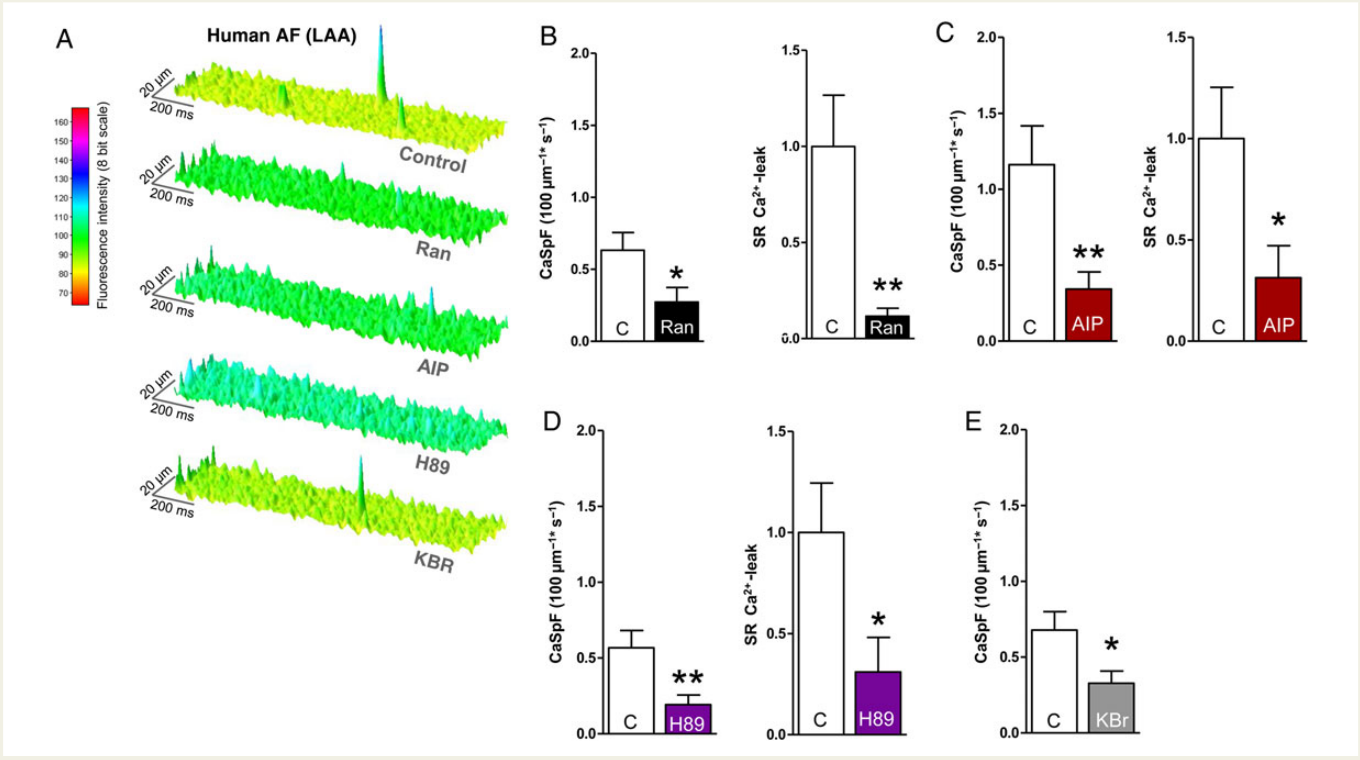

Figure 8 Effects of late I_{Na}, CaMKII, and PKA inhibition on SR-Ca^{2+}-leak in left atrial CMs of AF patients. (*A*) Surface plot of representative confocal line scans. Mean values of CaSpF and SR-Ca^{2+}-leak after treatment with (*B*) Ranolazine (*n* patients/cells = 5/100 vs. 5/71), (*C*) AIP (*n* = 4/44 vs. 4/34), (*D*) H89 (*n* = 4/95 vs. 4/78), and (*E*) KBR (*n* = 5/124 vs. 5/120, $P < 0.01$). *significant vs. control; $^{*/\#}P < 0.05$; $^{**/\#\#}P < 0.01$; $^{***/\#\#\#}P < 0.001$.

in CMs, which maintains CaMKII activation and includes positive feedback on SR-Ca^{2+}-leak and late I_{Na}.

4.3 Late I_{Na} increases cellular cAMP levels and activates PKA

PKA is also known to regulate RyR2 properties and was suggested to be involved in the disruption of diastolic RyR2 closure found in AF.[13] When PKA was inhibited in the setting of an increased late I_{Na}, we could successfully prevent the induction of SR-Ca^{2+}-leak. Thus, activation of PKA seems to be equally essential for the late I_{Na}-dependent induction of the SR-Ca^{2+}-leak. Indeed, the western blot data demonstrate that the PKA-specific target sites at PLN (S16) and RyR2 (S2808) are hyperphosphorylated in ATX-II-treated atrial myocardium. The fact that PKA is activated by cytoplasmic Na^+ influx via late I_{Na} has, to the best of our knowledge, not yet been described—either in atrial or in ventricular CMs—and further corroborates the link between Na^+ currents and cellular Ca^{2+}-cycling properties. Whereas the activation of CaMKII by Na^+-induced cellular Ca^{2+} overload is rather expected, nothing is known about the mechanism of Na^+-dependent PKA activation. PKA is an integral part of the β-adrenergic signalling pathway and is known to be activated by cAMP. We show that an enhancement of late I_{Na} by ATX-II induces a significant decrease of the measured YFP/CFP ratio in EPAC-camps transgenic mice,[14] indicating an increase in cytoplasmic cAMP levels. The change in YFP/CFP ratio during ATX-II-treatment was pronounced as it made up for ~28% of the maximal response upon β-adrenergic stimulation and can thus sufficiently explain PKA activation. We further used inhibitors of cardiac PDEs and ACs to elucidate if the late I_{Na}- related increase in cytoplasmic cAMP levels results from an inhibition of cardiac PDEs or an activation of ACs. Interestingly, preincubation with the unspecific PDE inhibitor IBMX did not block the cAMP response upon ATX-II treatment, showing that ATX-II does not exert its effect on cAMP levels by influencing PDE activity. In contrast, pre-inhibition of AC5 and 6 (the major cardiac AC isoforms) with NKY80[15] clearly attenuated the cAMP response upon ATX-II. Thus, the enhanced late I_{Na} by ATX-II increases cytoplasmic cAMP levels

by activating ACs. The fact that reverse-mode NCX inhibitor KBR also reduced ATX-II-dependent production of cAMP suggests a Ca^{2+}-dependent activation of ACs.

4.4 Late I_{Na}-dependent activation of CaMKII and PKA exerts differential effects on Ca^{2+} cycling properties

The confocal microscopy and western blot data show that late I_{Na} activates CaMKII and PKA and that inhibition of either kinase can effectively prevent the late I_{Na}-dependent induction of SR-Ca^{2+}-leak. SR-Ca^{2+}-leak is, however, not only dependent on the properties of diastolic RyR2 closure, but also on SR-Ca^{2+}-load (driving force). Surprisingly, late I_{Na} induction by ATX-II does not significantly influence systolic Ca^{2+}-transient amplitude or SR-Ca^{2+}-load compared to untreated control despite the markedly increased SR-Ca^{2+}-leak, suggesting simultaneously increased Ca^{2+} reuptake into the SR. When CaMKII, however, was additionally inhibited (AIP) or knocked-out (CaMKIIδc-KO mice), an enhanced late I_{Na} increased Ca^{2+}-transient amplitude and SR-Ca^{2+}-load. These findings clearly suggest that another mechanism, independent of CaMKII, must be activated by late I_{Na} in atrial CMs, which maintains SR-Ca^{2+}-load in the setting of an increased SR-Ca^{2+}-leak and even augments SR-Ca^{2+}-load when SR-Ca^{2+}-leak is simultaneously suppressed via inhibition of CaMKII. We hypothesized that PKA is most likely responsible for this effect. Indeed, atrial CMs treated with H89 in addition to ATX-II showed both, decreased Ca^{2+}-transient amplitude and decreased SR-Ca^{2+}-load compared to untreated control or sole ATX-II treatment. Furthermore, we detected a deceleration of Ca^{2+} reuptake into the SR ($k_{sys} - k_{caff}$) upon PKA inhibition. PKA thus enhances SR-Ca^{2+}-uptake in atrial CMs—most likely by SERCA2a disinhibition through PLN phosphorylation,[23] as demonstrated in the western blot experiments. In line with this interpretation, the rate of Ca^{2+} reuptake into the SR ($k_{sys} - k_{caff}$) was found to be accelerated when late I_{Na} was increased and CaMKII was inhibited (ATX-II + AIP). The fact that late I_{Na} induction alone (ATX-II) did not accelerate Ca^{2+} reuptake into the SR may well be explained by the significantly higher SR-Ca^{2+}-leak in this group counteracting cytosolic Ca^{2+} clearance by SERCA2a. The activation of SERCA2a by late I_{Na} can thus be unmasked by additional CaMKII inhibition that suppresses the increased SR-Ca^{2+}-leak. Furthermore, fractional release is increased by ATX-II despite formally unchanged systolic Ca^{2+}-transient amplitude and SR-Ca^{2+}-load, which can effectively be prevented by H89 but not by AIP. It can thus be attributed to PKA-dependent phosphorylation of RyR2 (S2808).

The current data elucidate the specific function of PKA and CaMKII in the induction of SR-Ca^{2+}-leak upon late I_{Na} activation and suggest that the mechanisms by which inhibition of CaMKII and PKA prevent SR-Ca^{2+}-leak may be different. As inhibition of CaMKII successfully prevents diastolic Ca^{2+}-leak-induction despite increased SR-Ca^{2+}-load, it can be assumed that CaMKII primarily alters RyR2 open probability in the setting of an increased late I_{Na} and CaMKII inhibition effectively suppresses diastolic RyR2 leakiness. The effect of CaMKII-dependent PLN-T17 phosphorylation on SERCA2a activity seems to be rather minor in atrial CMs as Ca^{2+} elimination kinetics are even accelerated upon an inhibition of CaMKII in the setting of an elevated late I_{Na}. This can be explained by the suppression of the CaMKII-induced SR-Ca^{2+}-leak that counteracts cytoplasmic Ca^{2+} clearance. In contrast, inhibition of PKA prevents the late I_{Na}-dependent diastolic leak induction in the setting of a decreased SR-Ca^{2+}-load. Thus, the reduced SR-Ca^{2+}-leak may only partly be explained by a lower PKA-dependent phosphorylation of RyR-S2808, but more likely by the decreased driving force for leak due to reduced SR-Ca^{2+}-reuptake. Importantly, the activity of both kinases is essential for the late I_{Na}-dependent induction of SR-Ca^{2+}-leak to occur. PKA thus facilitates CaMKII-dependent SR-Ca^{2+}-leak induction by maintaining SR-Ca^{2+}-load.

4.5 Inhibition of CaMKII, PKA, and late I_{Na} reduces SR-Ca^{2+}-leak in human AF

Slowed inactivation of I_{Na} has been reported in a canine model of chronic AF,[24] and we have recently shown that late I_{Na} is also enhanced in atrial CMs from patients with AF.[6] Moreover, we and others have demonstrated that SR-Ca^{2+}-leak is elevated in human AF and can be reduced by CaMKII inhibition.[11,12] We sought to find out whether the newly established mechanism of a cellular interdependence between late I_{Na} and SR-Ca^{2+}-leak can be applied to human AF. Therefore, we evaluated the effects of late I_{Na}, CaMKII, and PKA inhibition on SR-Ca^{2+}-leak in CMs from patients with permanent AF. Indeed, inhibition of CaMKII by AIP as well as inhibition of PKA with H89 reduced diastolic RyR2 leakiness. This confirms the involvement of both kinases and the translatability of the mechanisms elucidated in murine atrial CMs to human AF. The fact that inhibition of reverse-mode NCX (KBR) also reduced CaSpF in human AF suggests a Ca^{2+}-dependent activation of PKA (via ACs) and CaMKII. Importantly, a reduction of SR-Ca^{2+}-leak can also be achieved by inhibition of late I_{Na} with Ranolazine confirming the importance of pathologic Na^+ influx as an upstream activator of protein kinases and subsequent SR-Ca^{2+}-leak induction. Thus, late I_{Na} inhibition could potentially be used as a treatment strategy to improve Ca^{2+} homeostasis in AF.

4.6 Limitations of the study

(i) The mouse dataset relies on an induction of late I_{Na} by ATX-II. This toxin has often been used for this purpose, mostly in ventricular CMs, and has been shown to delay Na^+ channel inactivation and consequently induce Ca^{2+} overload.[25,26] In our current study, ATX-II concentration was titrated to yield an increase of late I_{Na} current in a range that is comparable to the magnitude found in cardiac disease and thus to approximate a previously healthy murine atrial CM to the compromised Na^+ gating found in human AF.[6] Although the translatability of our results is shown by the fact that inhibition of the respective kinases as well as of late I_{Na} successfully suppresses SR-Ca^{2+}-leak in human AF, unspecific actions of ATX-II cannot be completely excluded. Ca^{2+} overload may play an important role regarding the effects of ATX-II. This, however, may equally apply to an endogenously increased late I_{Na}. (ii) The calculation of spark size was performed by multiplying spark width by spark duration and amplitude. This calculation has repeatedly been used before.[27] It incorporates the main features of spontaneous Ca^{2+} release and enables a valid comparison of SR-Ca^{2+}-leak between groups relative to each other. However, a distinct absolute amount of Ca^{2+} loss cannot be inferred from this calculation. (iii) The observation of unchanged SR-Ca^{2+}-load upon late I_{Na} induction is based on CMs that were prestimulated at 1 Hz. Changes in SR loading at higher frequencies cannot be completely excluded. (iv) There is evidence in the literature about the existence of a non-spark SR-Ca^{2+}-leak.[28,29] Although we did not directly measure the non-spark leak in our present study, this would most likely not change its significance as currently available data suggest that it coexists with Ca^{2+}-spark-mediated

SR-Ca^{2+}-leak, and that both forms of diastolic Ca^{2+}-loss are apparently not altered independently in certain cell types and diseases.[29] Further studies investigating the non-spark-related leak in relation to late I_{Na} current and CaMKII/PKA activity may nevertheless be useful. However, Ca^{2+} sparks and waves may be of particular relevance as they constitute potent arrhythmogenic triggers. (v) BDM was used during murine cell isolation to increase cell quality and cell yield due to a reduction in actin–myosin interaction and ATP consumption. There are, however, concerns about BDM acting as a chemical phosphatase. As these side effects were shown to be dose-dependent,[30] we used a very low concentration of BDM (10 mmol/L). At this concentration, no significant effects of BDM on protein phosphorylation could be detected.[19] (vi) The use of caffeine in combination with Fluo dyes is an established method but might lead to some quenching of the indicator. This effect should be equally present in all groups and is known to be Ca^{2+}-dependent. Therefore, the detected differences in SR-Ca^{2+}-load would, if anything, rather be underestimated in this study.

4.7 Clinical relevance

Our data support the potentially high antiarrhythmic potency of late I_{Na} inhibition as this approach reduces SR-Ca^{2+}-leak in murine and human atrial CMs by interfering with the activity of CaMKII and PKA, both of which are known to exert deleterious effects in human cardiac disease. Inhibition of late I_{Na} appears to be a feasible way to control CaMKII activity in atrial myocardium and may overcome the current lack of cardiac-specific and clinically applicable CaMKII inhibitors. As CaMKII is crucially involved in neuronal processes, a systemic CaMKII inhibition could produce severe neurological side effects. Furthermore, our data show that inhibition of late I_{Na} as a therapeutic approach not only reduces CaMKII activation, but also interferes with the cAMP–PKA system and thus includes effects usually attributed to β-blockers. Of note, Ranolazine is currently being evaluated in clinical trials as a new treatment option for patients with AF (RAFFAELO Trial, EudraCT no.: 2011-002789-18, HARMONY Trial, EudraCT no.: 2011-001134-42) and new, even more selective and potent late I_{Na} inhibitors are currently under both experimental and clinical investigation (e.g. GS-6615; NCT01847391).

5. Summary

The dataset presented in this study shows that enhancement of late I_{Na} in atrial CM exerts significant effects on Ca^{2+} homeostasis. It leads to an NCX-dependent activation of CaMKII and an AC-mediated increase in cytoplasmic cAMP levels with subsequent activation of PKA. This results in hyperphosphorylation of the respective target sites at RyR2 and PLN and triggers a significant increase in SR-Ca^{2+}-leak. Importantly, activation of both CaMKII and PKA is necessary for increased SR-Ca^{2+}-leak to occur in the atria. Owing to the fact that SR-Ca^{2+}-reuptake is simultaneously facilitated, increased SR-Ca^{2+}-leak does not alter SR-Ca^{2+}-load. Increased SR-Ca^{2+}-turnover, however, is potentially highly arrhythmogenic. The increased diastolic SR-Ca^{2+}-leak in human AF can effectively be reduced by CaMKII inhibition as well as by inhibition of late I_{Na}.

Supplementary material

Supplementary material is available at *Cardiovascular Research* online.

Acknowledgements

We gratefully acknowledge the technical assistance of T. Schulte, K. Hansing, and T. Sowa.

Conflict of interest: L.S.M. receives research grants from Gilead and is involved in clinical trials with Gilead and Menarini. S.S. and L.S.M. receive speaker's honoraria from Berlin-Chemie. L.B., P.F., and L.Y. are employees of Gilead Sciences, Inc.

Funding

L.S.M., S.S., and G.H. are funded by the Deutsche Forschungsgemeinschaft (DFG) through the SFB 1002. S.S. is supported by the German Heart Foundation/German Foundation of Heart Research through a research grant. Funding to pay the Open Access publication charges for this article was provided by the Deutsche Forschungsgemeinschaft (DFG) through the SFB 1002.

References

1. Coraboeuf E, Deroubaix E, Coulombe A. Effect of tetrodotoxin on action potentials of the conducting system in the dog heart. *Am J Physiol* 1979;**236**:H561–H567.
2. Sossalla S, Wagner S, Rasenack EC, Ruff H, Weber SL, Schondube FA, Tirilomis T, Tenderich G, Hasenfuss G, Belardinelli L, Maier LS. Ranolazine improves diastolic dysfunction in isolated myocardium from failing human hearts—role of late sodium current and intracellular ion accumulation. *J Mol Cell Cardiol* 2008;**45**:32–43.
3. Ju YK, Saint DA, Gage PW. Hypoxia increases persistent sodium current in rat ventricular myocytes. *J Physiol* 1996;**497**(Pt 2):337–347.
4. Ward CA, Giles WR. Ionic mechanism of the effects of hydrogen peroxide in rat ventricular myocytes. *J Physiol* 1997;**500**(Pt 3):631–642.
5. Maltsev VA, Silverman N, Sabbah HN, Undrovinas AI. Chronic heart failure slows late sodium current in human and canine ventricular myocytes: implications for repolarization variability. *Eur J Heart Fail* 2007;**9**:219–227.
6. Sossalla S, Kallmeyer B, Wagner S, Mazur M, Maurer U, Toischer K, Schmitto JD, Seipelt R, Schondube FA, Hasenfuss G, Belardinelli L, Maier LS. Altered Na^+ currents in atrial fibrillation effects of ranolazine on arrhythmias and contractility in human atrial myocardium. *J Am Coll Cardiol* 2010;**55**:2330–2342.
7. Belardinelli L, Shryock JC, Fraser H. Inhibition of the late sodium current as a potential cardioprotective principle: effects of the late sodium current inhibitor ranolazine. *Heart* 2006;**92**(Suppl 4):iv6–iv14.
8. Kiyosue T, Arita M. Late sodium current and its contribution to action potential configuration in guinea pig ventricular myocytes. *Circ Res* 1989;**64**:389–397.
9. Song Y, Shryock JC, Belardinelli L. A slowly inactivating sodium current contributes to spontaneous diastolic depolarization of atrial myocytes. *Am J Physiol Heart Circ Physiol* 2009;**297**:H1254–H1262.
10. Wit AL, Boyden PA. Triggered activity and atrial fibrillation. *Heart Rhythm* 2007;**4**:S17–S23.
11. Neef S, Dybkova N, Sossalla S, Ort KR, Fluschnik N, Neumann K, Seipelt R, Schondube FA, Hasenfuss G, Maier LS. CaMKII-dependent diastolic SR Ca^{2+} leak and elevated diastolic Ca^{2+} levels in right atrial myocardium of patients with atrial fibrillation. *Circ Res* 2010;**106**:1134–1144.
12. Voigt N, Li N, Wang Q, Wang W, Trafford AW, Abu-Taha I, Sun Q, Wieland T, Ravens U, Nattel S, Wehrens XH, Dobrev D. Enhanced sarcoplasmic reticulum Ca^{2+} leak and increased Na^+-Ca^{2+} exchanger function underlie delayed afterdepolarizations in patients with chronic atrial fibrillation. *Circulation* 2012;**125**:2059–2070.
13. Vest JA, Wehrens XH, Reiken SR, Lehnart SE, Dobrev D, Chandra P, Danilo P, Ravens U, Rosen MR, Marks AR. Defective cardiac ryanodine receptor regulation during atrial fibrillation. *Circulation* 2005;**111**:2025–2032.
14. Calebiro D, Nikolaev VO, Gagliani MC, de Filippis T, Dees C, Tacchetti C, Persani L, Lohse MJ. Persistent cAMP-signals triggered by internalized G-protein-coupled receptors. *PLoS Biol* 2009;**7**:e1000172.
15. Brand CS, Hocker HJ, Gorfe AA, Cavasotto CN, Dessauer CW. Isoform selectivity of adenylyl cyclase inhibitors: characterization of known and novel compounds. *J Pharmacol Exp Ther* 2013;**347**:265–275.
16. Wasserstrom JA, Sharma R, O'Toole MJ, Zheng J, Kelly JE, Shryock J, Belardinelli L, Aistrup GL. Ranolazine antagonizes the effects of increased late sodium current on intracellular calcium cycling in rat isolated intact heart. *J Pharmacol Exp Ther* 2009;**331**:382–391.
17. Sipido KR, Callewaert G, Carmeliet E. Inhibition and rapid recovery of Ca^{2+} current during Ca^{2+} release from sarcoplasmic reticulum in guinea pig ventricular myocytes. *Circ Res* 1995;**76**:102–109.
18. Isenberg G, Ravens U. The effects of the Anemonia sulcata toxin (ATX II) on membrane currents of isolated mammalian myocytes. *J Physiol* 1984;**357**:127–149.
19. Fischer TH, Herting J, Tirilomis T, Renner A, Neef S, Toischer K, Ellenberger D, Forster A, Schmitto JD, Gummert J, Schondube FA, Hasenfuss G, Maier LS,

Sossalla S. Ca^{2+}/calmodulin-dependent protein kinase II and protein kinase A differentially regulate sarcoplasmic reticulum Ca^{2+} leak in human cardiac pathology. *Circulation* 2013;**128**:970–981.
20. Yao L, Fan P, Jiang Z, Viatchenko-Karpinski S, Wu Y, Kornyeyev D, Hirakawa R, Budas GR, Rajamani S, Shryock JC, Belardinelli L. $Na_v1.5$-dependent persistent Na^+ influx activates CaMKII in rat ventricular myocytes and N1325S mice. *Am J Physiol Cell Physiol* 2011;**301**:C577–C586.
21. Iwamoto T, Watano T, Shigekawa M. A novel isothiourea derivative selectively inhibits the reverse mode of Na^+/Ca^{2+} exchange in cells expressing NCX1. *J Biol Chem* 1996; **271**:22391–22397.
22. Wagner S, Dybkova N, Rasenack EC, Jacobshagen C, Fabritz L, Kirchhof P, Maier SK, Zhang T, Hasenfuss G, Brown JH, Bers DM, Maier LS. Ca^{2+}/calmodulin-dependent protein kinase II regulates cardiac Na^+ channels. *J Clin Invest* 2006;**116**:3127–3138.
23. Fujii J, Maruyama K, Tada M, MacLennan DH. Expression and site-specific mutagenesis of phospholamban. Studies of residues involved in phosphorylation and pentamer formation. *J Biol Chem* 1989;**264**:12950–12955.
24. Yagi T, Pu J, Chandra P, Hara M, Danilo P Jr, Rosen MR, Boyden PA. Density and function of inward currents in right atrial cells from chronically fibrillating canine atria. *Cardiovasc Res* 2002;**54**:405–415.
25. Hoey A, Harrison SM, Boyett MR, Ravens U. Effects of the Anemonia sulcata toxin (ATX II) on intracellular sodium and contractility in rat and guinea-pig myocardium. *Pharmacol Toxicol* 1994;**75**:356–365.
26. Fraser H, Belardinelli L, Wang L, Light PE, McVeigh JJ, Clanachan AS. Ranolazine decreases diastolic calcium accumulation caused by ATX-II or ischemia in rat hearts. *J Mol Cell Cardiol* 2006;**41**:1031–1038.
27. Zhang T, Guo T, Mishra S, Dalton ND, Kranias EG, Peterson KL, Bers DM, Brown JH. Phospholamban ablation rescues sarcoplasmic reticulum Ca^{2+} handling but exacerbates cardiac dysfunction in $CaMKIIdelta_C$ transgenic mice. *Circ Res* 2010;**106**: 354–362.
28. Brochet DX, Xie W, Yang D, Cheng H, Lederer WJ. Quarky calcium release in the heart. *Circ Res* 2011;**108**:210–218.
29. Bovo E, Mazurek SR, Blatter LA, Zima AV. Regulation of sarcoplasmic reticulum Ca^{2+} leak by cytosolic Ca^{2+} in rabbit ventricular myocytes. *J Physiol* 2011;**589**: 6039–6050.
30. Stapleton MT, Fuchsbauer CM, Allshire AP. BDM drives protein dephosphorylation and inhibits adenine nucleotide exchange in cardiomyocytes. *Am J Physiol* 1998;**275**: H1260–H1266.